Journal of Sound and Vibration (2001) **247**(4), 633–653
doi:10.1006/jsvi.2001.3769, available online at http://www.idealibrary.com on IDEAL®

ANALYTICAL STUDY OF A SYSTEM WITH A MECHANICAL FILTER

Y.-Y. Li and B. Balachandran

Department of Mechanical Engineering, University of Maryland, College Park, MD 20742-3035, *U.S.A.*

(*Received* 26 *June* 2000, *and in final form* 6 *April* 2001)

In the authors' earlier work, a concept called a *mechanical filter* was introduced and investigated for suppressing non-linear, planar crane–load oscillations on floating platforms. To implement this concept, the pivot point about which the load oscillations occur was constrained to follow a circular track. In the current effort, the geometry of the planar mechanical filter is generalized, and the corresponding non-linear dynamical system is derived and presented. On the basis of a Lyapunov function, analytical results are obtained to aid the choice of the filter geometry and the control law. For weak harmonic disturbances, the method of multiple scales is used to study non-linear oscillations of the system with a circular filter. The results of the perturbation analysis demonstrate the occurrence of cyclic-fold bifurcations in the system with the passive filter and suppression of crane–load oscillations in the system with the active filter. The analytical results are found to be in agreement with the associated numerical results. For large magnitude harmonic and aperiodic disturbances, numerical results demonstrate the effectiveness of the active filter in suppressing "large" crane–load oscillations. Tailoring of the response suppression bandwidth by using the active filter is also discussed.

1. INTRODUCTION

Cranes play an important role in production processes and serve to transfer loads from one place to another. Over the past several decades, the topic of safe and effective control of cranes on fixed and floating platforms has been addressed by numerous researchers. For a crane, which is mounted on a floating platform such as a shipboard crane, the disturbances produced by the platform motions also need to be taken into account.

The disturbances experienced by a ship vessel are usually aperiodic in nature, and in response, this vessel can undergo roll, surge, heave, yaw, sway, and pitch motions. For a shipboard crane, these vessel motions in turn excite the crane–load motions. In general, the dynamics of the three-dimensional load motions is complex (e.g., see references [1–3]). However, the dominant contribution in the disturbance provided to a crane load is known to be due to ship–roll motions. Although many studies on control of crane–load oscillations have been conducted previously, the focus of these studies has been on cranes on fixed platforms (e.g., references [4–10]). Furthermore, as discussed in the previous work of the authors [11–14], the above-mentioned efforts are primarily suited for control of "small" crane–load oscillations. Chin and Nayfeh [15] used perturbation analysis and numerical simulations to investigate a weakly non-linear model of a spherical pendulum representative of a ship–crane load. Yuan *et al.* [16] proposed a modified cable rigging called "Maryland Rigging" for controlling planar-load oscillations. Iwasaki *et al.* [17] used an active mass–damper system to attenuate oscillations of a sling frame, which is mounted on a floating crane.

0022-460X/01/440633 + 21 $35.00/0

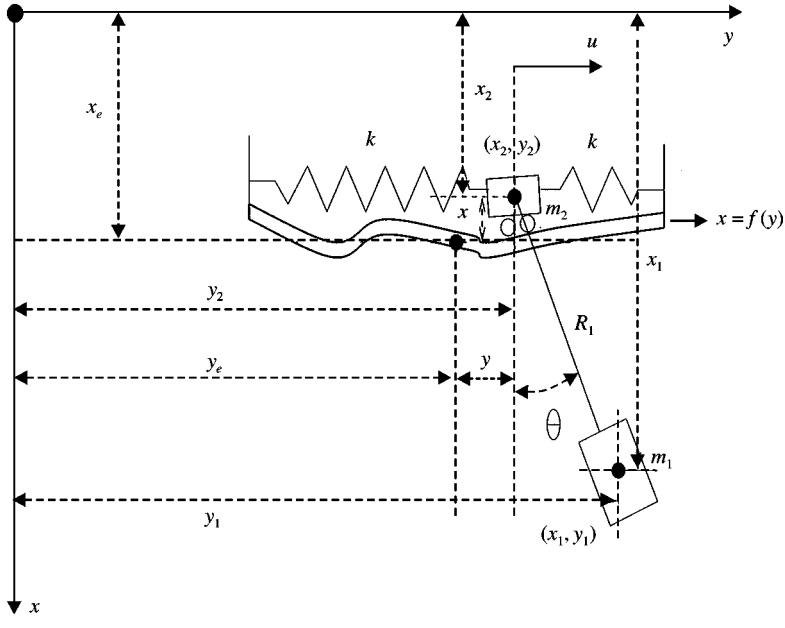

Figure 1. Planar system with generalized filter.

Recently, the notion of a mechanical filter was introduced for controlling non-linear, planar-load oscillations on floating platforms. As stated in the earlier efforts of the authors [11, 13], the words *mechanical filter* are used to mean a device that is introduced to suppress and/or eliminate undesired system dynamics. Here, the filter geometry is generalized and analytical results obtained by using a Lyapunov function and perturbation analysis are discussed. The numerical results are also presented to complement the analytical results and illustrate the effectiveness of the filter in the presence of "large" magnitude harmonic and aperiodic ship–roll-induced disturbances.

The rest of this paper is organized as follows. The governing equations for a system with the generalized filter are derived and presented in section 2 along with analytical results based on Lyapunov stability. For "weak" harmonic forcing, the method of multiple scales is used to analyze the non-linear oscillations of the system with the circular filter in section 3. In this section, numerical results obtained for "large" magnitude harmonic and aperiodic disturbances are also presented, and the influence of each of the different feedback terms on the load response is also explored. Inferences drawn from the work are presented to close the article.

2. MECHANICAL FILTER WITH GENERALIZED GEOMETRY

In this section, a planar mechanical filter with generalized geometry is considered as shown in Figure 1. The function $x = f(y)$, which describes the geometry of the track, is assumed to be a continuously differentiable function with respect to y upto the second order. The mass of the pivot is represented by m_2, the spring constant associated with each restraining spring is represented by k, and the dimensions of the pivot mass are assumed to be "small" with respect to characteristic dimensions of the track. The excitation components along the x- and y-axis are represented by x_e and y_e respectively.

For this system, after inclusion of damping and the control input u shown in Figure 1, the governing equations for the planar system are determined by using Lagrange's equations to have the following form:

$$m_1R_1^2\ddot{\theta} + m_1R_1\left[-\ddot{x}_e\sin\theta + (\ddot{y} + \ddot{y}_e)\cos\theta - \frac{\mathrm{d}f}{\mathrm{d}y}\sin\theta\ddot{y} - \frac{\mathrm{d}^2f}{\mathrm{d}y^2}\sin\theta\dot{y}^2\right] + m_1gR_1\sin\theta + c_\theta\dot{\theta} = 0, \tag{1}$$

$$m_1R_1\ddot{\theta}\left(-\frac{\mathrm{d}f}{\mathrm{d}y}\sin\theta + \cos\theta\right) + m_1R_1\dot{\theta}^2\left(-\frac{\mathrm{d}f}{\mathrm{d}y}\cos\theta - \sin\theta\right) + (m_1 + m_2)\frac{\mathrm{d}f}{\mathrm{d}y}\ddot{x}_e + (m_1 + m_2)\left[1 + \left(\frac{\mathrm{d}f}{\mathrm{d}y}\right)^2\right]\ddot{y} + (m_1 + m_2)\ddot{y}_e - (m_1 + m_2)g\frac{\mathrm{d}f}{\mathrm{d}y} + (m_1 + m_2)\frac{\mathrm{d}f}{\mathrm{d}y}\frac{\mathrm{d}^2f}{\mathrm{d}y^2}\dot{y}^2 + c_y\dot{y} + 2ky = u. \tag{2}$$

Once the geometry of the track is chosen as in the study of Balachandran *et al.* [13], the governing equations of the system can be obtained by substituting the geometry function $f(y)$ into equations (1) and (2). This function can be chosen to introduce "appropriate" coupling non-linearities between the pivot state y and the load state θ. In these equations, the quantities c_θ and c_y represent damping associated with the angular motions of the load and the horizontal translational motions of the pivot point respectively. Next, to aid the choice of the track geometry and the form of the active control law, analytical results obtained on the basis of a Lyapunov function are presented.

Theorem 1. *Suppose that* $x_e = y_e = 0$ *and* $c_\theta = c_y = 0$ *in dynamical system* (1) *and* (2) *and let the filter geometry be such that* $x = f(y) \leqslant 0$, *and the control input* $u = -B\dot{y}$, $B > 0$. *Also, let the origin* $(\theta, \dot{\theta}, y, \dot{y}) = (0, 0, 0, 0)$ *be the considered equilibrium point and* $D \subset S \times R^3$ *be a domain containing the equilibrium point. Then, the equilibrium position* $(\theta, \dot{\theta}, y, \dot{y}) = (0, 0, 0, 0)$ *is stable.*

Proof. Let the energy function of the system be chosen as the Lyapunov function; that is,

$$V = \tfrac{1}{2}m_1(\dot{x}_1^2 + \dot{y}_1^2) + \tfrac{1}{2}m_2(\dot{x}_2^2 + \dot{y}_2^2) + R_1(1 - \cos\theta)m_1g - x(m_1 + m_2)g + ky^2. \tag{3}$$

From equation (3), it is clear that

$$V(0) = 0 \quad \text{and} \quad V > 0 \quad \text{in } D - \{0\}. \tag{4}$$

The time derivative $\dot{V}$ along a solution of equations (1) and (2) is given by

$$\dot{V} = (m_1 + m_2)\left\{\frac{\mathrm{d}f(y)}{\mathrm{d}y}\frac{\mathrm{d}^2f(y)}{\mathrm{d}y^2}\dot{y}^3 + \left[\left(\frac{\mathrm{d}f(y)}{\mathrm{d}y}\right)^2 + 1\right]\dot{y}\ddot{y}\right\} + m_1R_1\left\{ -\frac{\mathrm{d}^2f(y)}{\mathrm{d}y^2}\dot{y}^2\dot{\theta}\sin\theta - \left[\frac{\mathrm{d}f(y)}{\mathrm{d}y}\sin\theta - \cos\theta\right](\dot{\theta}\ddot{y} + \dot{y}\ddot{\theta})\right.$$

$$-\left[\frac{\mathrm{d}f(y)}{\mathrm{d}y}\cos\theta + \sin\theta\right]\dot{y}\dot{\theta}^2 + R_1\dot{\theta}\ddot{\theta}\Bigg\}$$

$$+ R_1\dot{\theta}\sin\theta m_1 g - \frac{\mathrm{d}f(y)}{\mathrm{d}y}\dot{y}(m_1 + m_2)g + 2ky\dot{y}. \tag{5}$$

After making use of equation (1), the expression for $\dot{V}$ can be simplified to

$$\dot{V} = u\dot{y} = -B\dot{y}^2 \leqslant 0 \quad \text{in } D - \{0\}. \tag{6}$$

Therefore, according to Lyapunov, the equilibrium point is stable [18, 19]. □

Theorem 2. *Suppose that* $x_e = y_e = 0$ *and* $c_\theta = c_y = 0$ *in the dynamical system* (1) *and* (2) *and let the filter geometry be such that* $x = f(y) \leqslant 0$ *and the control input* $u = -B\dot{y}$, $B > 0$. *If there is no other solution* $(\theta^*, \dot{\theta}^*, y^*, \dot{y}^*)$ *of system* (1) *and* (2) *under the above conditions other than the solution* $(\theta, \dot{\theta}, y, \dot{y}) = (0, 0, 0, 0)$ *within* $D_l \subset D \subset S \times R^3$, *then the origin* $(\theta, \dot{\theta}, y, \dot{y}) = (0, 0, 0, 0)$ *is asymptotically stable in* D_l.

Proof. From Lyapunov function (3), one has $V(0) = 0$, and a domain can be found so that

$$D_l = \{(\theta, \dot{\theta}, y, \dot{y}) | V \leqslant l\}, \tag{7}$$

where l is a finite positive quantity. In addition,

$$V > 0 \quad \text{for } (\theta, \dot{\theta}, y, \dot{y}) \in D_l \quad \text{and} \quad (\theta, \dot{\theta}, y, \dot{y}) \neq (0, 0, 0, 0), \tag{8}$$

$$\dot{V} = u\dot{y} = -B\dot{y}^2 \leqslant 0 \quad \text{for } (\theta, \dot{\theta}, y, \dot{y}) \in D_l. \tag{9}$$

On the basis of Krasovskii's theorem [18], the origin $(\theta, \dot{\theta}, y, \dot{y}) = (0, 0, 0, 0)$ is asymptotically stable in D_l. □

It is easy to verify that the above two theorems hold when $c_\theta > 0$ and $c_y > 0$. From the above global analytical results, as expected, it is found that the derivative feedback term $B\dot{y}$ plays an important role in determining the system stability. Regarding the geometry of the filter, the results indicate that as long as $x = f(y) \leqslant 0$, it is possible to have a stable non-linear system. Shapes other than a circular track that satisfy this condition can be used. However, the analytical results presented thus far are valid only for free oscillations. In the case of harmonically forced oscillations, the Lyapunov function can still be used to illustrate response stabilization.

3. MECHANICAL FILTER WITH CIRCULAR GEOMETRY

In this section, a mechanical filter with a circular track is presented along with results of non-linear analysis carried out for a system subjected to a "weak" harmonic forcing. A linear analysis is also presented to illustrate how the system resonances can be tailored by using active feedback. In addition, the system responses are numerically explored for "large" magnitude excitations and the influences of the different feedback terms on the load response are also explored.

In Figure 2, side views of a crane configuration and a modified crane configuration are shown along with an enlarged inset of the filter introduced in the earlier work of the authors

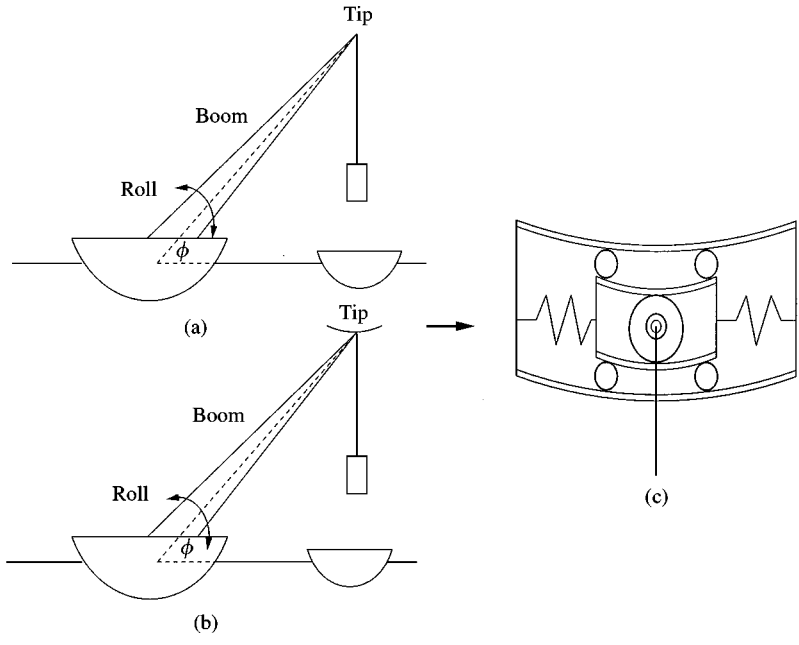

Figure 2. Crane configuration without rider block tagging system: filter at boom tip. (a) Sideview of crane configuration; (b) modified crane configuration, (c) mechanical filter.

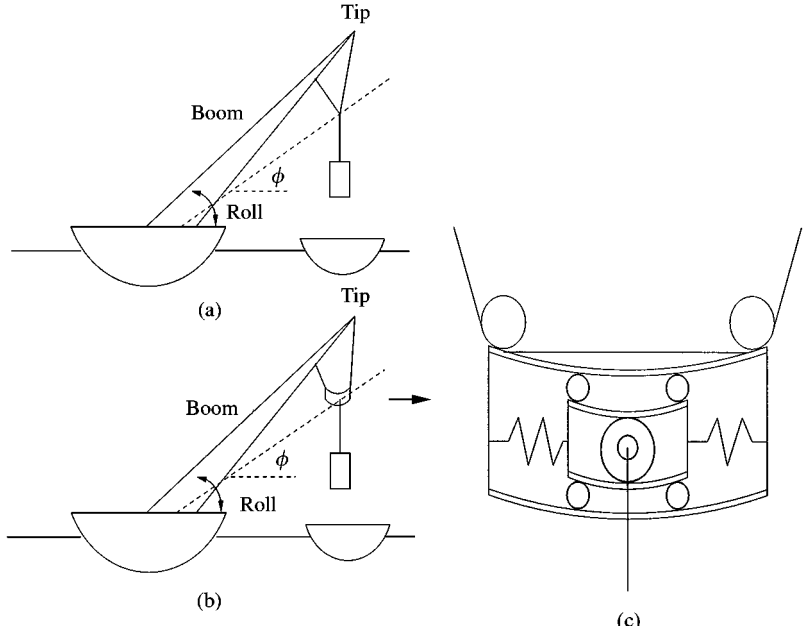

Figure 3. Crane configuration with rider block tagging system: filter in-between boom tip and load. (a) Sideview of crane configuration; (b) modified crane configuration; (c) mechanical filter.

[13, 14]. In Figure 3, side views of a different crane configuration and a modified version of this crane configuration are shown along with an enlarged inset of the circular filter. In the crane systems shown in Figures 2 and 3, the mechanical filters are installed at two different

positions. In each case, the boom orientation in the plane is specified by the angle ϕ and the longitudinal axis of the vessel about which the roll oscillations occur is normal to the considered side view. Here, only planar-load oscillations that may arise as a result of ship–roll motions are addressed. Although the physical configurations shown in Figures 2 and 3 are different, the same mathematical model can be used to describe the systems with and without the filter to understand the qualitative aspects of the dynamics.

Assuming that the boom configuration is rigid, the roll motion of the ship will translate into an excitation with horizontal and vertical components at the crane pivot. As in the earlier work [13], the circular track is assumed to be of radius R_2. After inclusion of damping, the planar pendulum in the system without the filter is governed by

$$m_1 R_1^2 \ddot{\theta} + m_1 R_1(-\ddot{x}_e \sin\theta + \ddot{y}_e \cos\theta) + m_1 g R_1 \sin\theta + c_\theta \dot{\theta} = 0, \tag{10}$$

where R_1 is the length of the inextensional cable shown in Figure 1.

In the system with the filter, the motion of mass m_2 is constrained to follow a circular track that is described by

$$x = -\frac{y^2}{2R_2} - \frac{y^4}{8R_2^3}. \tag{11}$$

After substituting equation (11) into equations (1) and (2), the resulting equations are

$$m_1 R_1^2 \ddot{\theta} + m_1 R_1 \left[-\ddot{x}_e \sin\theta + (\ddot{y} + \ddot{y}_e)\cos\theta + \left(\frac{y}{R_2} + \frac{y^3}{2R_2^3}\right)\sin\theta \ddot{y} + \left(\frac{1}{R_2} + \frac{3y^2}{2R_2^3}\right)\sin\theta \dot{y}^2 \right] + m_1 g R_1 \sin\theta + c_\theta \dot{\theta} = 0, \tag{12}$$

$$\begin{aligned} &m_1 R_1 \ddot{\theta}\left[\left(\frac{y}{R_2} + \frac{y^3}{2R_2^3}\right)\sin\theta + \cos\theta\right] + m_1 R_1 \dot{\theta}^2 \left[\left(\frac{y}{R_2} + \frac{y^3}{2R_2^3}\right)\cos\theta - \sin\theta\right] \\ &- (m_1 + m_2)\left(\frac{y}{R_2} + \frac{y^3}{2R_2^3}\right)\ddot{x}_e + (m_1 + m_2)\left[1 + \left(\frac{y}{R_2} + \frac{y^3}{2R_2^3}\right)^2\right]\ddot{y} \\ &+ (m_1 + m_2)\ddot{y}_e + (m_1 + m_2) g \left(\frac{y}{R_2} + \frac{y^3}{2R_2^3}\right) \\ &+ (m_1 + m_2)\left(\frac{y}{R_2} + \frac{y^3}{2R_2^3}\right)\left(\frac{1}{R_2} + \frac{3y^2}{2R_2^3}\right)\dot{y}^2 + c_y \dot{y} + 2ky = u. \end{aligned} \tag{13}$$

When the excitation due to the roll motion of the vessel is harmonic, the excitation components $x_e(t)$ and $y_e(t)$ can be idealized to be

$$x_e(t) = (F \sin \Omega t)\cos\phi, \qquad y_e(t) = (F \sin \Omega t)\sin\phi, \tag{14}$$

where F is the excitation amplitude and Ω is the excitation frequency. To simulate excitations produced by aperiodic roll motions, the Rössler system (e.g., reference [16])

$$\left.\begin{aligned} \dot{x} &= -0{\cdot}5(y + z) \\ \dot{y} &= 0{\cdot}5(x + ay) \\ \dot{z} &= 0{\cdot}5[b + z(x - c)] \end{aligned}\right\} \quad x_e = 0{\cdot}2x\cos\phi; \quad y_e = 0{\cdot}2x\sin\phi \tag{15}$$

with the parameter values $a = 0{\cdot}398$, $b = 2$, and $c = 4$ is used.

In the system with the filter, when the control input $u = 0$ in equations (12) and (13), the corresponding case is referred to as a "passive control" or "passive filter" case. Otherwise, the corresponding case is referred to as an "active control" or "active filter" case. As in the study of Balachandran *et al.* [13], a feedback control law of the following form is considered.

$$u = u_{feedback} = m_1(A \sin\theta + B\dot{y} + Cy). \tag{16}$$

3.1. LINEAR SYSTEM

Here, a linearized version of equations (12) and (13) is used to point out how the proportional feedback terms in the active control law (16) can be used to tailor the system resonances. For "small" oscillations of the system about the trivial equilibrium position $(\theta, \dot{\theta}, y, \dot{y}) = (0, 0, 0, 0)$, when $x_e = y_e = 0$, $c_\theta = c_y = 0$, and $B = 0$, equations (12) and (13) can be linearized to, respectively, obtain

$$m_1 R_1^2 \ddot{\theta} + m_1 R_1 \ddot{y} + m_1 g R_1 \theta = 0, \tag{17}$$

$$m_1 R_1 \ddot{\theta} + (m_1 + m_2)\ddot{y} + (m_1 + m_2) g \frac{y}{R_2} + 2ky = u = m_1(A\theta + Cy). \tag{18}$$

The resonances associated with coupled system (17) and (18) are

$$\omega_{1,2}^2 = \frac{\left[\dfrac{m_1 + m_2}{m_2} g\left(\dfrac{1}{R_1} + \dfrac{1}{R_2}\right) + \dfrac{m_1}{m_2 R_1} A + \left(\dfrac{2k}{m_2} - \dfrac{m_1}{m_2} C\right)\right]}{2}$$

$$\pm \frac{\sqrt{\left[\dfrac{m_1 + m_2}{m_2} g\left(\dfrac{1}{R_1} + \dfrac{1}{R_2}\right) + \dfrac{m_1}{m_2 R_1} A + \left(\dfrac{2k}{m_2} - \dfrac{m_1}{m_2} C\right)\right]^2 - 4g\left[\dfrac{m_1 + m_2}{m_2 R_1} \dfrac{g}{R_2} + \left(\dfrac{2k}{m_2} - \dfrac{m_1}{m_2} C\right)\right]}}{2}. \tag{19}$$

With the assumption that ω_2 is larger than ω_1, it is seen from equation (19) that when C is chosen so that $(m_1 + m_2)m_2 R_1\, g/R_2 + (2k/m_2 - (m_1/m_2)C)$ is close to zero, the system can have two distinct natural frequencies ω_1 and ω_2. Of these values, ω_1 is close to zero and ω_2 can be a "large" value when A is "large". Therefore, the two natural frequencies of the system can be controlled by appropriately choosing the values of A and C in the static feedback control law.

For example, when $m_1/m_2 = 100$, $R_1 = 9{\cdot}8$ m, $k = 0$, and $R_2 = 20$ m, the first natural frequency ω_1 and the second natural frequency ω_2 can be calculated from equation (19) to be 0·70 and 14·12 rad/s respectively. On increasing the track radius R_2 from 10 to 50 m, ω_1 is shifted to 0·40 rad/s and ω_2 is shifted to 10·98 rad/s. It is mentioned that ω_2 is high enough to be out of the excitation frequency range of interest and ω_1 can be further shifted to a low value by increasing the track radius.

3.2. NON-LINEAR SYSTEM

In this subsection, the method of multiple scales (e.g., reference [20]) is used to obtain an analytical approximation for the solution of equations (12) and (13) in the presence of

"weak" harmonic excitations. For local oscillations about the trivial equilibrium position, retaining upto cubic non-linearities, these equations can be used to obtain

$$\ddot{y} = \left\{ m_1 \left(-\frac{y\theta}{R_2} + \frac{\theta^2}{2} - 1 \right) \left[-\frac{\dot{y}^2\theta}{R_2} - g\left(\theta - \frac{\theta^3}{6}\right) - \frac{c_\theta}{m_1 R_1}\dot{\theta} - \ddot{y}_e\left(1 - \frac{\theta^2}{2}\right) \right] \right.$$
$$+ m_1 \left(-\frac{y\theta}{R_2} + \frac{\theta^2}{2} - 1 \right) \left[\ddot{x}_e \left(\theta - \frac{\theta^3}{6}\right) \right] - (m_1 + m_2)\frac{y}{R_2}\ddot{x}_e - (m_1 + m_2)\ddot{y}_e$$
$$+ m_1 R_1 \dot{\theta}^2 \left(-\frac{y}{R_2} + \theta \right) + (m_1 + m_2)\left(-\frac{y}{R_2} \right) g - (m_1 + m_2)\left(\frac{y}{R_2^2}\dot{y}^2 \right)$$
$$\left. - c_y\dot{y} - 2ky + u \right\} \Big/ m_2 \left[1 + \frac{y^2}{R_2^2} + \frac{m_1}{m_2}\left(\theta^2 + \frac{y^2}{R_2^2} - 2\frac{y\theta}{R_2} \right) \right], \tag{20}$$

$$\ddot{\theta} = \left(-\frac{y\theta}{R_2} + \frac{\theta^2}{2} - 1 \right) \left\{ m_1 \left(-\frac{y\theta}{R_2} + \frac{\theta^2}{2} - 1 \right) \left[-\frac{\dot{y}^2\theta}{R_2} - g\left(\theta - \frac{\theta^3}{6}\right) - \frac{c_\theta}{m_1 R_1}\dot{\theta} \right] \right.$$
$$+ m_1 \left(-\frac{y\theta}{R_2} + \frac{\theta^2}{2} - 1 \right) \left[\ddot{x}_e \left(\theta - \frac{\theta^3}{6}\right) - \ddot{y}_e \left(1 - \frac{\theta^2}{2}\right) \right]$$
$$- (m_1 + m_2)\ddot{y}_e - (m_1 + m_2)\frac{y}{R_2}\ddot{x}_e$$
$$+ m_1 R_1 \dot{\theta}^2 \left(-\frac{y}{R_2} + \theta \right) + (m_1 + m_2)\left(-\frac{y}{R_2} \right) g - (m_1 + m_2)\frac{y}{R_2^2}\dot{y}^2$$
$$\left. - c_y\dot{y} - 2ky + u \right\} \Big/ R_1 m_2 \left[1 + \frac{y^2}{R_2^2} + \frac{m_1}{m_2}\left(\theta^2 + \frac{y^2}{R_2^2} - 2\frac{y\theta}{R_2} \right) \right]$$
$$+ \frac{1}{R_1}\left[\left(-\frac{1}{R_2} \right)\dot{y}^2\theta - g\left(\theta - \frac{\theta^3}{6}\right) - \frac{c_\theta}{m_1 R_1}\dot{\theta} - \ddot{y}_e\left(1 - \frac{\theta^2}{2}\right) + \ddot{x}_e\left(\theta - \frac{\theta^3}{6}\right) \right]. \tag{21}$$

An approximate solution of equations (20) and (21) is sought by using the method of multiple scales. In order to facilitate the perturbation analysis, a small dimensionless parameter ε is introduced as a book-keeping device to make explicit that certain terms are "small". At the end of the analysis, this parameter is set equal to one. Two time scales are introduced according to

$$T_0 = t \quad \text{and} \quad T_2 = \varepsilon^2 t. \tag{22}$$

In addition, for the passive filter, the parameter $k = 0$ and the control input $u = 0$. Weak harmonic excitations, weak damping, and small ratio of pivot mass to crane–load mass are realized by introducing

$$x_e(t) = \varepsilon^3 F_x \cos \Omega t \quad \text{and} \quad y_e(t) = \varepsilon^3 F_y \cos \Omega t, \tag{23}$$

$$\frac{c_\theta}{m_2 R_1} = \varepsilon^3 \mu_\theta \quad \text{and} \quad \frac{c_y}{m_2} = \varepsilon^3 \mu_y \tag{24}$$

and

$$\frac{m_2}{m_1} = O(\varepsilon^2). \tag{25}$$

An analytical approximation for the solution of equations (20) and (21) is sought in the form

$$y(t) = \varepsilon y_1(T_0, T_2) + \varepsilon^3 y_3(T_0, T_2) + \cdots,$$

$$\theta(t) = \varepsilon\theta_1(T_0, T_2) + \varepsilon^3\theta_3(T_0, T_2) + \cdots. \tag{26}$$

After substituting equation (26) into equations (20) and (21) and equating coefficients of like powers of ε, the following hierarchy of equations is obtained:

$O(\varepsilon)$:

$$D_0^2 y_1 + \left(\frac{m_1 + m_2}{m_2}\right)\frac{g}{R_2}\, y_1 - \frac{m_1}{m_2}\, g\theta_1 = 0,$$

$$D_0^2\theta_1 - \left(\frac{m_1 + m_2}{m_2 R_1}\right)\frac{g}{R_2}\, y_1 + \frac{m_1 + m_2}{m_2 R_1}\, g\theta_1 = 0. \tag{27}$$

$O(\varepsilon^3)$:

$$\begin{aligned} D_0^2 y_3 + \left(\frac{m_1 + m_2}{m_2}\right)\frac{g}{R_2}\, y_3 - \frac{m_1}{m_2}\, g\theta_3 \\ = -2D_0D_2(y_1) - F_y\Omega^2\cos(\Omega t) + \mu_\theta D_0\theta_1 - \mu_y D_0 y_1 \\ + \frac{m_1}{m_2 R_2}\theta_1\,(D_0 y_1)^2 - \frac{m_1 R_1}{m_2 R_2}\, y_1 (D_0\theta_1)^2 \\ + \frac{m_1 R_1}{m_2}\,\theta_1 (D_0\theta_1)^2 - \frac{m_1}{m_2 R_2^2}\, y_1\,(D_0 y_1)^2 \\ - \frac{m_1^2}{m_2^2}\, g\theta_1^3 + \frac{m_1(3m_1 + m_2)}{m_2^2}\,\frac{g}{R_2}\, y_1\theta_1^2 \\ - \frac{m_1(3m_1 + m_2)}{m_2^2}\,\frac{g}{R_2^2}\, y_1^2\theta_1 + \frac{m_1(m_1 + m_2)}{m_2^2}\,\frac{g}{R_2^3}\, y_1^3, \end{aligned}$$

$$\begin{aligned} D_0^2\theta_3 - \left(\frac{m_1 + m_2}{m_2 R_1}\right)\frac{g}{R_2}\, y_3 + \left(\frac{m_1 + m_2}{m_2 R_1}\right) g\theta_3 \\ = -2D_0D_2(\theta_1) + \frac{\mu_y}{R_1}\, D_0 y_1 - \frac{\mu_\theta}{R_1}\, D_0\theta_1 \\ - \frac{(m_1/m_2 + 1)}{R_1 R_2}\theta_1\,(D_0 y_1)^2 + \frac{m_1}{m_2 R_2}\, y_1 (D_0\theta_1)^2 \end{aligned}$$

$$-\frac{m_1}{m_2}\theta_1(D_0\theta_1)^2+\frac{m_1}{m_2R_1R_2^2}y_1(D_0y_1)^2$$

$$+\frac{m_1^2}{m_2^2R_1}g\theta_1^3-\frac{m_1(3m_1+m_2)}{m_2^2}\frac{g}{R_2R_1}y_1\theta_1^2$$

$$+\frac{m_1(3m_1+m_2)}{m_2^2}\frac{g}{R_2^2R_1}y_1^2\theta_1-\frac{m_1(m_1+m_2)}{m_2^2}\frac{g}{R_2^3R_1}y_1^3. \tag{28}$$

On examining the first of equations (28), it is noticeable that the external excitation directly excites only the y motion after the introduction of the filter. This aspect is illustrative of the filtering action of the mechanical filter.

The solution of equation (27) can be expressed in the form

$$y_1(T_0, T_2)=A_1(T_2)\exp(\mathrm{i}\omega_1T_0)+A_2(T_2)\exp(\mathrm{i}\omega_2T_0)+\mathrm{cc},$$

$$\theta_1(T_0, T_2)=\Lambda_1A_1(T_2)\exp(\mathrm{i}\omega_1T_0)+\Lambda_2A_2(T_2)\exp(\mathrm{i}\omega_2T_0)+\mathrm{cc}, \tag{29}$$

where the A_i are complex-valued amplitudes, cc indicates the complex conjugate of the preceding terms, the quantities ω_n^2 are the roots of

$$\begin{vmatrix} -\omega^2+\dfrac{m_1+m_2}{m_2}\dfrac{g}{R_2} & -\dfrac{m_1}{m_2}g \\ -\dfrac{m_1+m_2}{m_2R_1}\dfrac{g}{R_2} & -\omega^2+\dfrac{m_1+m_2}{m_2R_1}g \end{vmatrix}=0 \tag{30}$$

and

$$\Lambda_n=\frac{(m_1+m_2)/m_2R_1\ g/R_2}{(m_1+m_2)/m_2R_1\ g-\omega_n^2}. \tag{31}$$

The frequencies ω_n, which are assumed to be distinct, depend upon the track radius R_2, the ratio of the pivot mass to the crane–load mass, and the cable length R_1, as pointed out in section 3.1. When the filter is active, they also depend upon the proportional feedback components.

At this stage, a detuning parameter σ is introduced to define the (primary) resonance

$$\Omega=\omega_1+\varepsilon^2\sigma \tag{32}$$

and it is noted that

$$\Omega t=\Omega T_0=(\omega_1+\varepsilon^2\sigma)T_0=\omega_1T_0+\sigma T_2. \tag{33}$$

Introducing $A_n=\frac{1}{2}\alpha_n\exp(\mathrm{i}\beta_n)$ with real-valued quantities α_n and β_n into equation (29) and considering the solvability conditions associated with equations (28) to eliminate the source of the secular terms, the following slow-scale equations are obtained:

$$-\omega_1\left(\frac{m_1+m_2}{m_2R_1}g-\omega_1^2+\frac{m_1}{m_2}g\Lambda_1\right)\alpha_1'+\left(\frac{m_1+m_2}{m_2R_1}g-\omega_1^2\right)\frac{F_y}{2}\omega_1^2\sin(\sigma T_2-\beta_1)$$

$$+\frac{1}{2}\omega_1\left\{\left(\frac{m_1+m_2}{m_2R_1}g-\omega_1^2\right)(\mu_\theta\Lambda_1-\mu_y)+\frac{m_1}{m_2}g\left[\frac{\mu_y}{R_1}-\frac{\mu_\theta\Lambda_1}{R_1}\right]\right\}\alpha_1=0,$$

$$\omega_1\alpha_1\left(\frac{m_1+m_2}{m_2R_1}g-\omega_1^2+\frac{m_1}{m_2}g\Lambda_1\right)\beta_1'+\left(\frac{m_1+m_2}{m_2R_1}g-\omega_1^2\right)\frac{F_y}{2}\omega_1^2\cos(\sigma T_2-\beta_1)$$

$$+\left(\frac{m_1+m_2}{m_2R_1}g-\omega_1^2-\frac{m_1g}{m_2R_1}\right)\bar{\Gamma}_1=0, \tag{34}$$

$$-\omega_2\left(\frac{m_1+m_2}{m_2R_1}g-\omega_2^2+\frac{m_1}{m_2}g\Lambda_2\right)\alpha_2'+\frac{1}{2}\omega_2\left\{\left(\frac{m_1+m_2}{m_2R_1}g-\omega_2^2\right)(\mu_\theta\Lambda_2-\mu_y)\right.$$

$$\left.+\frac{m_1}{m_2}g\left[\frac{\mu_y}{R_1}-\frac{\mu_\theta\Lambda_2}{R_1}\right]\right\}\alpha_2=0,$$

$$\omega_2\alpha_2\left(\frac{m_1+m_2}{m_2R_1}g-\omega_2^2+\frac{m_1}{m_2}g\Lambda_2\right)\beta_2'+\left(\frac{m_1+m_2}{m_2R_1}g-\omega_2^2-\frac{m_1g}{m_2R_1}\right)\bar{\Gamma}_2=0, \tag{35}$$

where

$$\bar{\Gamma}_1=-\frac{m_1^2}{m_2^2}g\left(\frac{3}{8}\Lambda_1^3\alpha_1^3+\frac{3}{4}\Lambda_1\Lambda_2^2\alpha_1\alpha_2^2\right)$$

$$+\frac{m_1(3m_1+m_2)}{m_2^2}\frac{g}{R^2}\left(\frac{3}{8}\Lambda_1^2\alpha_1^3+\frac{1}{4}\Lambda_2^2\alpha_1\alpha_2^2+\frac{1}{2}\Lambda_1\Lambda_2\alpha_1\alpha_2^2\right)$$

$$-\frac{m_1(3m_1+m_2)}{m_2^2}\frac{g}{R_2^2}\left(\frac{3}{8}\Lambda_1\alpha_1^3+\frac{1}{4}\Lambda_1\alpha_1\alpha_1^2+\frac{1}{2}\Lambda_2\alpha_1\alpha_2^2\right)$$

$$+\frac{m_1(m_1+m_2)}{m_2^2}\frac{g}{R_2^3}\left(\frac{3}{8}\alpha_1^3+\frac{3}{4}\alpha_1\alpha_2^2\right). \tag{36}$$

The expression for $\bar{\Gamma}_2$ is identical to equation (36) except that Λ_1 is replaced by Λ_2, Λ_2 is replaced by Λ_1, α_1 is replaced by α_2, and α_2 is replaced by α_1. Furthermore, in arriving at equations (34) and (35), only the dominant cubic non-linearities have been retained for simplification [14].

When the active input

$$u=\varepsilon^3m_1B\dot{y} \tag{37}$$

is included, the resulting slow-scale or modulation equations are identical in form to equations (34) and (35) except that μ_y is replaced by $\bar{\mu}_y$, which is given by

$$\bar{\mu}_y=\mu_y-\frac{m_1}{m_2}B. \tag{38}$$

From equation (35), it is found that the asymptotic response of the amplitude α_2 goes to zero when (positive) damping is present. Hence, for further analysis, only equation (34) is considered.

To generate numerical results for the system, the cable length R_1 is chosen to be 9·8 m, the radius of the track R_2 is set to 10 m, the mass ratio $m_1/m_2=100$, and the damping quantities are set to $c_\theta/m_1R_1=0{\cdot}04$ and $c_y/m_1=0$. The excitation amplitude is chosen to be 0·2015 m. Fixed-point solutions of equation (34) and periodic solutions of equations (12)

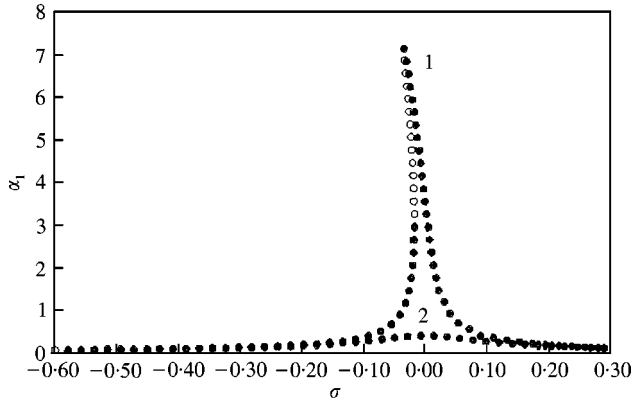

Figure 4. Perturbation results for amplitude α_1 versus detuning parameter σ for two different values of damping.

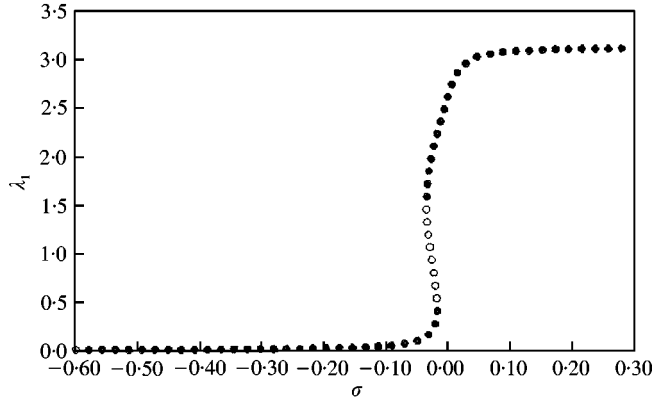

Figure 5. Phase $\lambda_1 = (\sigma T_2 - \beta_1)$ versus detuning parameter σ.

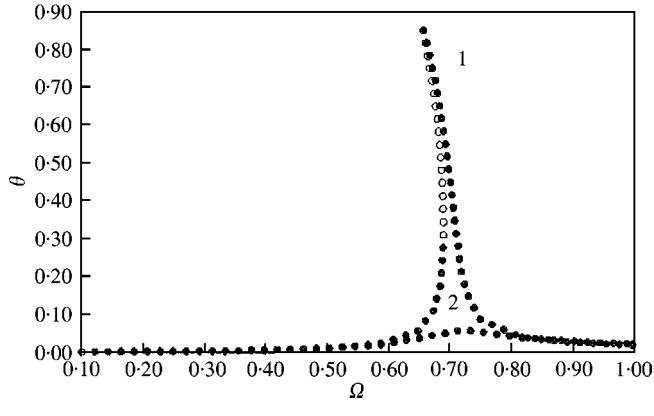

Figure 6. Numerical results for amplitude θ versus excitation frequency $\Omega = \omega_1 + \sigma$.

and (13) are determined by using AUTO94. The results obtained when the excitation frequency is used as a control parameter are shown in Figures 4–6. The stable solutions are represented by solid circles, and the unstable solutions are represented by open circles.

In Figures 4 and 5, the amplitude α_1 and the associated phase $\lambda_1 = (\sigma T_2 - \beta_1)$ are shown respectively. The curve labelled 1 in Figure 4 corresponds to the case when $u = 0$ and the curve labelled 2 in Figure 4 corresponds to the case when $u \neq 0$ and $B = -0{\cdot}5$. The phase response is only shown for $u = 0$. In the passive filter case, a softening-spring-type response is discernible along with the presence of saddle-node bifurcations (fold bifurcations in the original system; that is, equations (20) and (21)). These bifurcations are eliminated with increase in the damping.

The numerical results obtained based on system (12) and (13) are shown in Figure 6. Noting that the magnitude of the state θ predicted by the perturbation analysis is approximately $\Lambda_1\alpha_1$, which is $0{\cdot}1005\ \alpha_1$ for the parameters chosen here, the agreement between the results of Figures 4 and 6 is found to be good.

To verify that saddle-node bifurcations do occur in the response curve labelled 1 in Figure 4, it was examined whether points of vertical tangencies occur at the bifurcation points. To this end, the following expression relating the amplitude α_1 to the detuning parameter σ is obtained from equation (34):

$$\frac{\mathrm{d}\sigma}{\mathrm{d}\alpha_1^2} = -\frac{(\omega_1 C_2\sigma + C_3\bar{\bar{\Gamma}}_1\alpha_1^2)^2 + \frac{1}{4}\omega_1 C_4^2}{2\alpha_1^2(\omega_1 C_2\sigma + C_3\bar{\bar{\Gamma}}_1\alpha_1^2)(\omega_1 C_2)} - \frac{C_3\bar{\bar{\Gamma}}_1}{\omega_1 C_2}, \tag{39}$$

where

$$C_1 = \frac{m_1 + m_2}{m_2 R_1} g - \omega_1^2, \qquad C_2 = C_1 + \frac{m_1}{m_2} g\Lambda_1, \qquad C_3 = C_1 - \frac{m_1 g}{m_2 R_1},$$

$$C_4 = C_1(\mu_\theta\Lambda_1 - \mu_y) + \frac{m_1}{m_2} g\left[\frac{\mu_y}{R_1} - \frac{\mu_\theta\Lambda_1}{R_1}\right],$$

$$\bar{\bar{\Gamma}}_1 = -\frac{m_1^2}{m_2^2} g\left(\frac{3}{8}\Lambda_1^3\right) + \frac{m_1(3m_1 + m_2)}{m_2^2}\frac{g}{R_2^2}\left(\frac{3}{8}\Lambda_1^2 R_2 - \frac{3}{8}\Lambda_1\right)$$

$$+ \frac{m_1(3m_1 + m_2)}{m_2^2}\frac{g}{R_2^3}\frac{3}{8}. \tag{40}$$

From equation (39), it is verified that [14]

$$\frac{\mathrm{d}\sigma}{\mathrm{d}\alpha_1^2} = 0 \tag{41}$$

confirming that the bifurcation points in Figure 4 correspond to points of vertical tangencies or tangent bifurcations (e.g., reference [18]). Further analysis has ruled out the possibility of Hopf bifurcations in the slow-scale equations [14].

3.3. LARGE MAGNITUDE EXCITATIONS

In the previous work of the authors [13], it was demonstrated that in the system with the passive filter, the bifurcations of the periodic responses are shifted to a different parameter range, and that in the system with the active filter, these bifurcations can be eliminated. The numerical results obtained for the active filter system are revisited here. In particular, the parameter values corresponding to this system are as follows. The boom orientation angle is 30°, the cable length R_1 is chosen to be 9·8 m, the mass ratio $m_1/m_2 = 0{\cdot}01$, and the damping

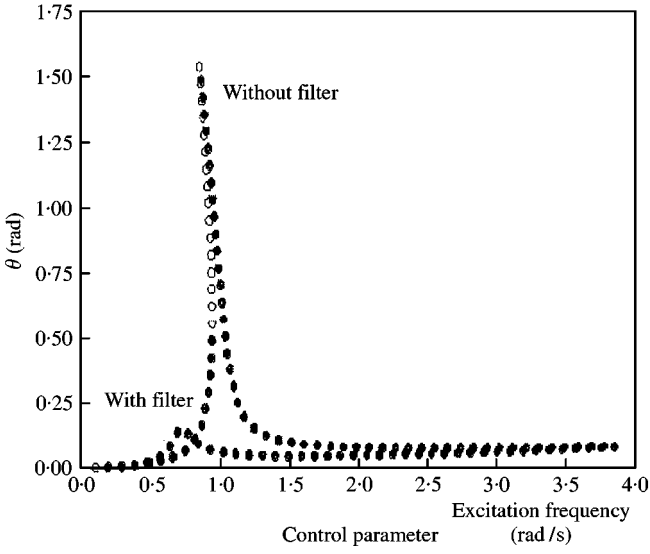

Figure 7. Responses with and without active filter: $R_2 = 10$ m.

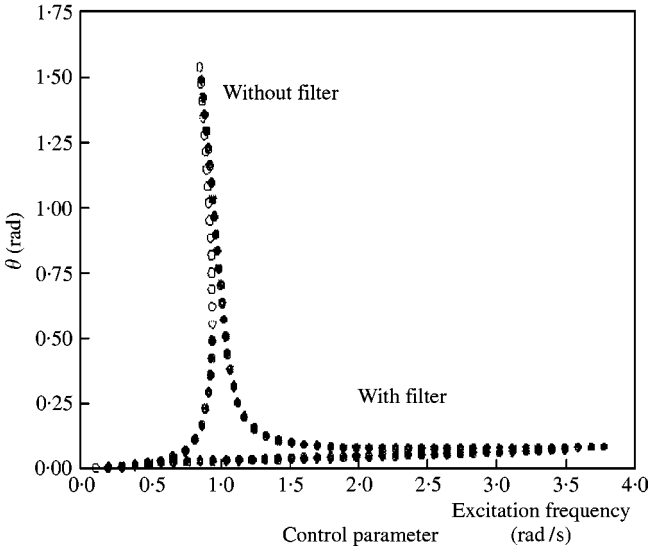

Figure 8. Responses with and without active filter: $R_2 = 50$ m.

quantities $c_0/m_1R_1 = 0{\cdot}02$ and $c_y/m_1 = 0{\cdot}0$. The excitation amplitude is fixed at 1 m. The track radius R_2 is 10 m in one case and 50 m in the other case. The parameters A, B, and C in the control law (16) are 96·22, $-0{\cdot}5$, and 0·0 respectively. The magnitudes of the stable and unstable responses obtained by using AUTO94 are shown in Figures 7 and 8.

From Figures 7 and 8, it is observed that the cyclic-fold bifurcations of the response of the load swing oscillation θ that occur in the absence of the filter are eliminated after introduction of the filter. Furthermore, by increasing the track radius, the magnitude of the load oscillation in the system with the filter is always less than that in the system without the filter over a wide range of the excitation frequency. In other words, the suppression

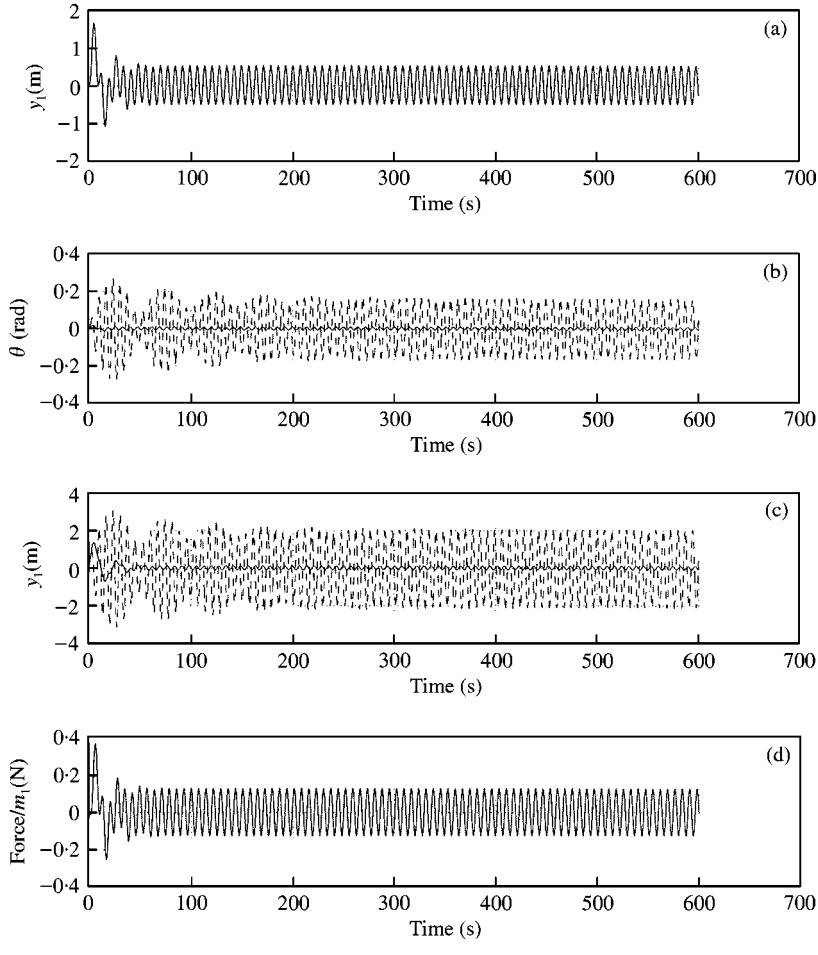

Figure 9. Time histories with active filter: (a) horizontal translation of the pivot; (b) angular position of the load; (c) horizontal translation of the load, and (d) force applied to pivot. - - - - -, lines correspond to absence of filter and ——, lines correspond to presence of filter.

bandwidth can be increased to the whole range by using the static feedback control law and increasing the track radius.

With reference to Figure 1, from a practical standpoint, one is likely to be concerned with attenuation of the load horizontal displacement y_1 rather than the angular displacement θ about the local position. In the system without the filter, the load horizontal displacement is given by

$$y_1 = y_e + R_1 \sin\theta \tag{42}$$

and in the system with the filter, the load horizontal displacement is given by

$$y_1 = y_e + y + R_1 \sin\theta. \tag{43}$$

To show that the load horizontal displacement is also effectively attenuated, a representative case with $A = 24{\cdot}06$, $B = -0{\cdot}5$, $C = 0{\cdot}0$, excitation frequency $\Omega = 0{\cdot}87$ rad/s, and excitation amplitude $F = 1$ m is considered. The respective time histories obtained through numerical integration of equations (12) and (13) are shown in Figure 9.

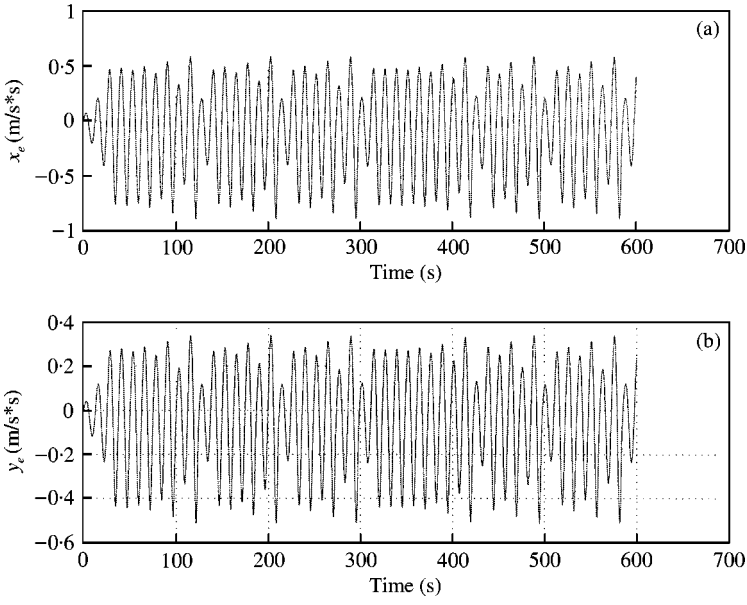

Figure 10. Time histories generated from Rössler system: (a) $\ddot{x}_e$ and (b) $\ddot{y}_e$.

In Figure 9, the time histories of the pivot motion(y), the load angular oscillation(θ), the swing motion(y_1), and the control force input to the pivot mass m_2 are provided. From Figure 9, it is evident that in the system with the filter, one can not only attenuate the load angular oscillation but also the swing oscillation. This can be explained as follows. Since, the y motion of the pivot is actuated to counteract the excitation y_e, from equation (43), it is clear that if $y = -y_e$, as the load oscillation amplitude goes to zero, the horizontal displacement of the load also goes to zero,

To examine the effectiveness of the active filter in the presence of an aperiodic disturbance, a representative case is considered. In this case, the aperiodic disturbance is simulated by using the *Rössler* system. As described by equations (15), the parameter values $a = 0{\cdot}398$, $b = 2{\cdot}0$, and $c = 4{\cdot}0$ are chosen to obtain chaotic motions and a scaling is used to generate x_e and y_e as in the work of Yuan *et al.* [16] The resulting time histories are shown in Figure 10.

The load responses in the absence and presence of the active filter are shown in Figure 11. Although the excitation has many frequency components, the system with the filter is effective in attenuating the load horizontal displacement. The filter parameters are $R_2 = 5$ m, $A = 0{\cdot}64$, $B = -4{\cdot}0$, and $C = 0{\cdot}0$.

3.4. INFLUENCE OF DIFFERENT FEEDBACK TERMS

Here, the influence of the different proportional terms and the velocity feedback terms on the load response is considered for harmonic excitations. The results are presented in the form of bifurcation diagrams generated by using AUTO94 with the excitation frequency being treated as a control parameter. The boom orientation angle, the cable length, and the mass ratio have the same values as in section 3.3. The excitation amplitude is fixed at 1 m.

In the system with the passive filter, as reported in the work of Li [14], even when the damping c_θ is increased to large values, bifurcations persist. However, in the system with

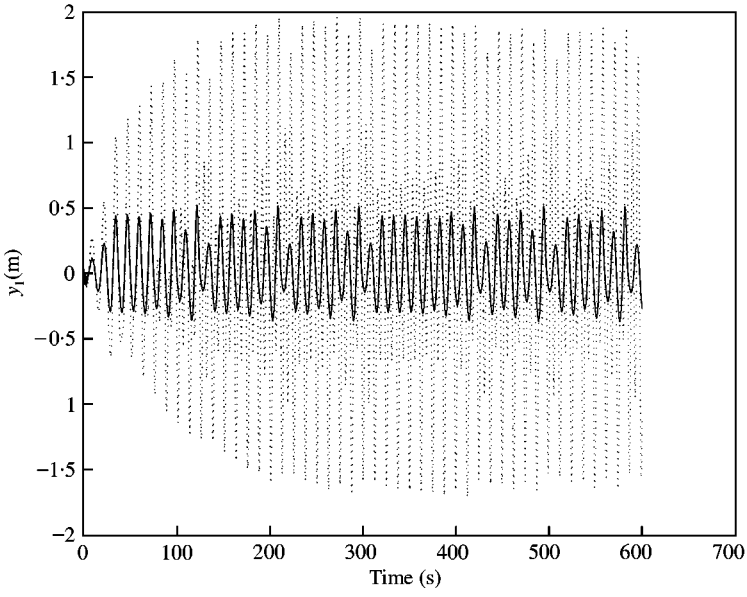

Figure 11. Load responses to aperiodic excitation: - - - - -, lines corresponds to absence of filter and ——, lines correspond to presence of filter.

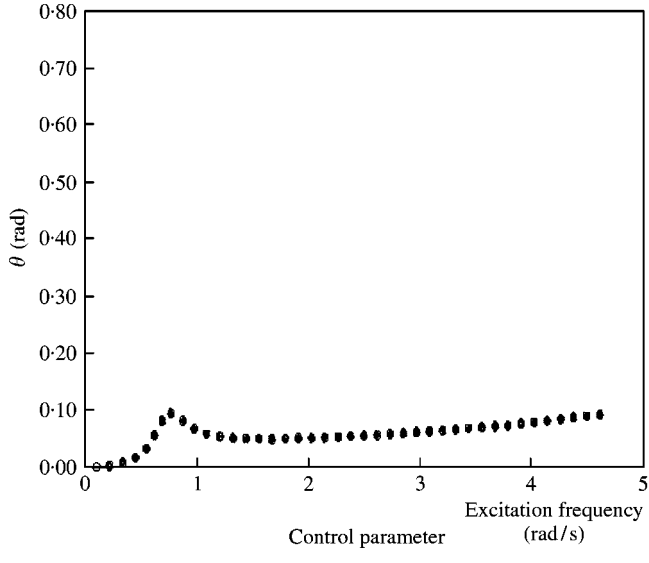

Figure 12. Responses with active filter: $u = -0{\cdot}8\dot{y}$.

the active filter, these bifurcations can be eliminated as discussed before and shown in Figures 12–16. To generate the results shown in Figure 12, the control law $u = -0{\cdot}8\dot{y}$ was used with $R_2 = 10\,\text{m}$. With only velocity feedback, the bifurcations can be eliminated. As pointed out in section 3.2, an increase in damping associated with the y motions is helpful in this regard.

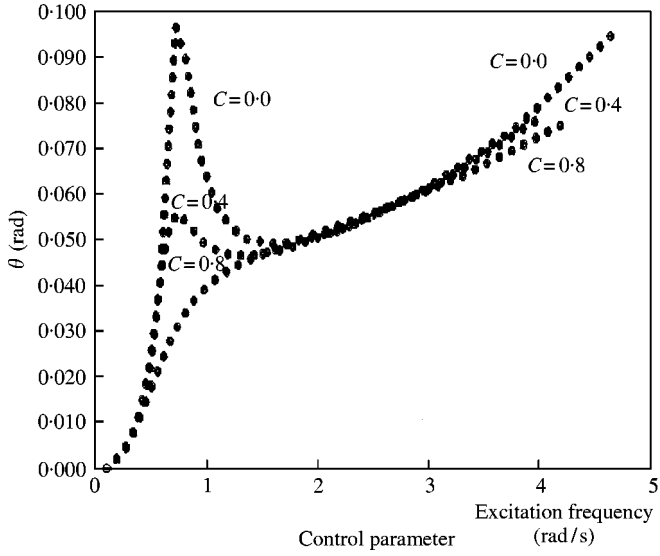

Figure 13. Responses with active filter: $u = -0{\cdot}8\dot{y} + Cy$. Three curves corresponding to the parameter values of 0·0, 0·4, and 0·8 for C are shown in the figure.

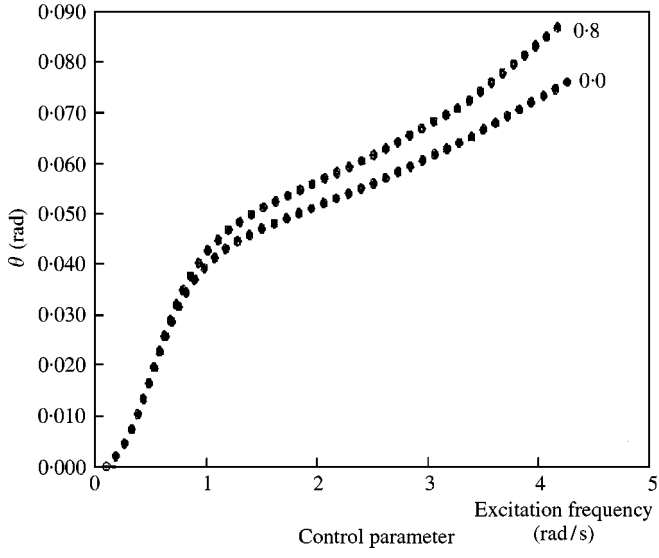

Figure 14. Responses with active filter: $u = -0{\cdot}8\dot{y} + 0{\cdot}8y$. Two curves corresponding to the parameter values of 0·0 and 0·8 for C_θ/m_1R_1 are shown in the figure.

To generate the results shown in Figure 13, a proportional feedback term associated with y motions is included in addition to the derivative feedback term used earlier. The corresponding coefficient is increased from 0·0 to 0·8. One may recall that, as discussed in section 3.1, the parameter C in control law (16) can be used to tailor the resonance locations. This is taken advantage of as C is increased to 0·8 to attenuate the load oscillations. In Figure 14, it is shown that regardless of the value of damping quantity c_θ (i.e., positive or zero), the control law with proportional feedback and derivative feedback associated with y motions is effective in suppressing the load oscillations over a wide frequency range.

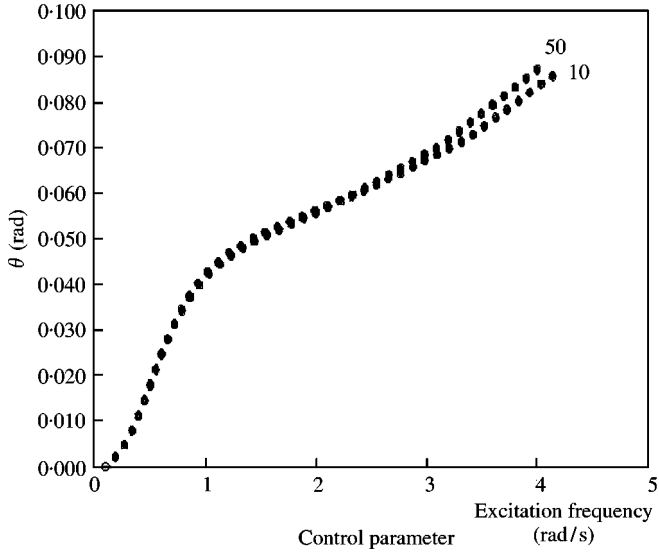

Figure 15. Responses with active filter: $R_2 = 10$ and 50 m.

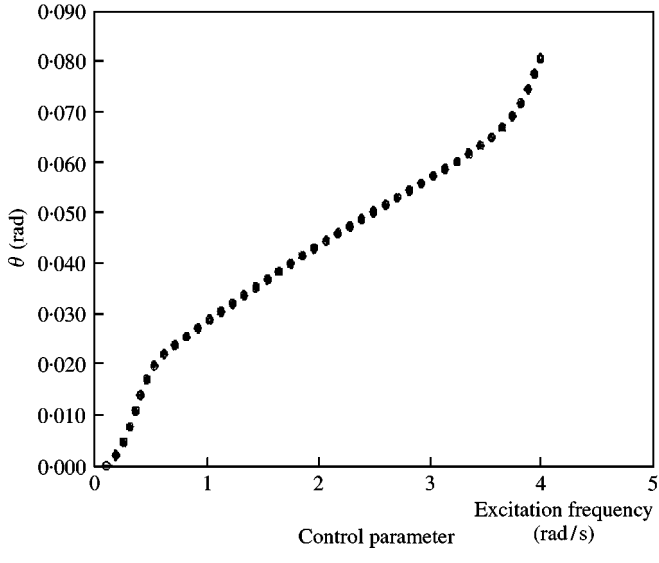

Figure 16. Responses with active filter: inputs u_1 and u_2. The two curves are virtually on top of each other.

To obtain the results shown in Figure 15, two different track radii are considered. For the system with the radius of 10 m, the control input $u = -0{\cdot}8\dot{y} + 0{\cdot}8y$ is used, and for the system with the radius of 50 m, the control input $u = -0{\cdot}8y$ is used. It is seen that with the inclusion of proportional feedback, even for a "smaller" track radius, the active filter is effective in load response attenuation.

In Figure 8 of section 3.2, the responses are shown for a case where the track radius is 50 m and the control input has the form $u = 96{\cdot}2361 \sin\theta - 0{\cdot}5\dot{y}$. For a shorter track radius of 10 m and $u_2 = 96{\cdot}2361 \sin\theta - 0{\cdot}5\dot{y} + 0{\cdot}8y$, the results obtained are shown in Figure 16.

Comparable results are obtained even if the non-linear proportional feedback term in θ is dropped and when the control input $u_1 = -0{\cdot}5\dot{y} + 0{\cdot}8y$ is used. The primary thrust of the results presented in section 3.4 has been that with a careful choice of velocity feedback and proportional feedback associated with y motions one can effectively eliminate bifurcations and enhance response suppression.

4. CONCLUDING REMARKS

The geometry of the planar mechanical filter introduced in an earlier work by the authors has been generalized in this work, and non-linear analyses has been carried out with the aid of a Lyapunov function and perturbation analysis. The analytical results obtained on the basis of the Lyapunov function show that shapes other than a circular track can also be used for the filter geometry and the importance of derivative feedback associated with pivot motions for system stability. The perturbation analysis conducted by using the method of multiple scales confirm the presence of cyclic-fold bifurcations and softening-type behavior in the frequency–response curves observed in the numerical results. For "large" amplitude harmonic and aperiodic excitations, the numerical results illustrate the effectiveness of the active filter in load response attenuation. It is also pointed out that the response suppression bandwidth can be tailored by suitably designing the control input.

ACKNOWLEDGMENTS

Support received for this work from the U.S. Office of Naval Research through contract No. N00014-96-1-1123 is gratefully acknowledged. Dr Kam Ng, the technical monitor for this work, is thanked for his valuable inputs.

REFERENCES

1. M. H. PATEL, D. T. BROWN and J. A. WITZ 1987 *Transactions of the Royal Institution of Naval Architects* **129**, 103–113. Operability analysis for a monohull crane vessel.
2. F. J. MCCORMICK and J. A. WITZ 1993 *Underwater Technology* **19**, 30–39. An investigation into the parametric excitation of suspended loads during crane vessel operations.
3. J. A. WITZ 1995 *Ocean Engineering* **22**, 411–420. Parametric excitation of crane loads in moderate sea states.
4. Y. SAKAWA and A. NAKAZUMI 1985 *Transactions of the American Society of Mechanical Engineers Journal of Dynamic Systems, Measurement, and Control* **107**, 200–206. Modeling and control of a rotary crane.
5. K. A. F. MOUSTAFA and A. M. EBEID 1988 *Transactions of the American Society of Mechanical Engineers Journal of Dynamic Systems, Measurement, and Control* **110**, 266–271. Nonlinear modeling and control of overhead crane load sway.
6. R. SOUISSI and A. J. KOIVO 1992 *First IEEE Conference on Control Applications, Dayton, OH*, 782–787. Modeling and control of a rotary crane for swing-free transport of payloads.
7. J. W. AUERNIG and H. TROGER 1987 *Automatica* **23**, 437–447. Time optimal control of overhead cranes with hoisting of the load.
8. B. d'ANDRÉA-NOVEL and J. LEVINE 1990 *Proceedings of the International Symposium MTNS-89* II, 523–529. Modelling and nonlinear control of an overhead crane.
9. M. FLEISS, J. LEVINE and P. ROUCHON 1991 *IEEE Proceedings of the* 30*th Conference on Decision and Control, Brighton, England*, 736–741. A simplified approach of crane control via a generalized state-space model.
10. G. G. PARKER, B. PETTERSON, C. R. DOHRMANN and R. D. ROBINETT 1995 *Proceedings of the Smart Structures and Materials* 1995 *Symposium on Industrial and Commercial Applications of Smart Structures Technologies, San Diegeo, CA*, Vol. 2447, 131–140. Vibration suppression of fixed-time jib crane maneuvers.

11. B. BALACHANDRAN and Y.-Y. LI 1997 *Proceedings of the DETC'97* 1997, *ASME Design Engineering Technical Conferences*, *Sacramento*, *CA*, September 14–17, Vol. DETC97/VIB-4091, 1–6. A mechanical filter concept to suppress crane–load oscillations.
12. Y.-Y. LI and B. BALACHANDRAN 1998 *Proceedings of the* 1998 *ASME International Mechanical Engineering Congress & Exposition*, *Anaheim*, *CA*, November 15–20, AD-Vol. 57/MD-Vol. 83, 203–208. Active control of shipboard cranes to suppress load vibrations.
13. B. BALACHANDRAN, Y.-Y. LI and C.-C. FANG 1999 *Journal of Sound and Vibration* **228**, 651–682. A mechanical filter concept for control of nonlinear oscillations.
14. Y.-Y. LI 1999 *Ph.D. Dissertation*, *University of Maryland at College Park*, *MD*. Mechanical filters for controlling crane–load oscillations.
15. C. CHIN and A. H. NAYFEH 1996 *Proceedings of the* 37*th AIAA/ASME/ASCE/AHS/ASC Structures*, *Structural Dynamics*, *and Materials Conference*, *Salt Lake City*, *UT*, April 15–17, Vol. AIAA Paper No. 96-1485. Nonlinear dynamics of crane operation at sea.
16. G.-H. YUAN, B. HUNT, C. GREBOGI, E. OTT, J. YORKE and E. KOSTELICH 1997 *Proceedings of the DETC'97* 1997 *ASME Design Engineering Technical Conferences*, *Sacramento*, *CA*, Vol. DETC97/VIB-4095. Design and control of shipboard cranes.
17. I. IWASAKI, K. TANIDA, S. KAJI and M. MUTAGUCHI 1997 *Proceedings of the DETC'97* 1997 *ASME Design Engineering Technical Conferences*, *Sacramento*, *CA*, Vol. DETC97/VIB-3816, 1–8. Development of an active mass damper for stabilizing the load suspended on a floating crane.
18. A. H. NAYFEH and B. BALACHANDRAN 1995 *Applied Nonlinear Dynamics*: *Analytical*, *Computational*, *and Experimental Methods*. New York: Wiley.
19. H. K. KHALIL 1996 *Nonlinear Systems*. Upper Saddle River, NJ: Prentice-Hall.
20. A. H. NAYFEH and D. T. MOOK 1979 *Nonlinear Oscillations*. New York: Wiley.